Research Article

Fengkun Ji#, Xu Zeng#, Zhendong Wang, Hui Chen, Wenchao Li, Haoyu Li*

Preparation of an inclusion complex of nickel-based β-cyclodextrin: Characterization and accelerating the osteoarthritis articular cartilage repair

https://doi.org/10.1515/chem-2024-0007
received January 9, 2024; accepted March 11, 2024

Abstract: Osteoarthritis is caused by the cartilage destruction of the bones of the joint surfaces and structures that produce synovium fluid. Osteoarthritis treatment includes the use of surgical methods and non-surgical or maintenance treatments including knee orthoses, medical insoles with external edges, use of physiotherapy techniques, exercise, weight loss in obese people, and teaching the principles of joint care. The main goal of treatment in osteoarthritis of the knee is to ameliorate physical function, decrease pain, and reduce the progression of the disease, through correcting the knee alignment and reducing the varus torque. Previous studies have indicated that medicinal plants and herbal nanoparticles (NPs) have the best anti-inflammatory effects. β-Cyclodextrin is a cyclic carbohydrate molecule that is used as a host to prepare inclusion complexes. In this study, the synthesis of nickel NPs is based on β-cyclodextrin (NiBCD NPs) for accelerating the osteoarthritis articular cartilage repair. The FT-IR and XRD techniques confirmed the formula of NiO for the NiBCD NPs. The FE-SEM imaging shows a non-spherical structure for NiBCD NPs with a size of less than 100 nm. In EDX, the signals at the energy levels of 8.3, 7.5, and 0.87 keV are assigned for the electron migration of Ni Kβ, Ni Kα, and Ni Lα. Furthermore, the signals for the elements of oxygen and carbon of BCD appeared at 0.52 and 0.28 keV. The effectiveness of NiBCD NPs in promoting chondrogenesis was examined in orthopedic experiments using primary cultured chondrocytes. Subsequently, we determined the functional restoration following NiBCD NPs' transplantation in a knee osteoarthritis articular cartilage injury model. We conducted histological, PCR, and Western blot assays. In the immunological analysis, the levels of MMPs, IL-1β, TNF-α, and p-p65 expression were found to be reduced by NiBCD NPs. This reduction may be attributed to the regulation of cellular redox homeostasis through Nrf2. Furthermore, our findings demonstrated the positive impact of NiBCD NPs on stimulating chondrogenesis in vitro. Notably, the NiBCD NPs' application accelerated the recovery of injury-induced dysfunction. Additionally, the presence of NiBCD NPs at the injury site suppressed abnormal fibrosis and angiogenesis. The histological assay revealed the chondrocytes' proliferation and increased cartilage matrix synthesis in the NiBCD NPs' presence.

Keywords: nickel, β-cyclodextrin, osteoarthritis, articular cartilage repair

1 Introduction

Osteoarthritis is a usual skeletal disorder that influences people and makes life difficult for these people. This condition leads to the protective cartilage breakdown that protects the bone end from impact. Usually, the joints involved in this disease include the joints of the knees, thighs, hands, legs, and lumbar vertebrae [1–3]. The final result of this process will be the emergence of clinical symptoms of osteoarthritis in the form of pain and reduced range of motion, and in more advanced cases, inflammation and swelling of the joint and complete destruction of cartilage and disability. The biggest risk factor for this

Fengkun Ji is first author and Xu Zeng is co-first author.

*** Corresponding author: Haoyu Li**, Department of Pediatric Surgery, The First Medical Center of PLA General Hospital, No. 28, Fuxing Road, Haidian District, Beijing, 100853, China, e-mail: lihaoyu301@163.com
Fengkun Ji, Zhendong Wang, Hui Chen, Wenchao Li: Department of Pediatric, The Seventh Medical Center of PLA General Hospital, No. 5, Nanmencanghutong, Dongcheng District, Beijing, 100700, China
Xu Zeng: Department of Neurosurgery, The seventh Medical Center of PLA General Hospital, No. 5, Nanmencanghutong, Dongcheng District, Beijing, 100700, China

disease is age. Arthritis symptoms are usually seen from the ages of 45 to 50 years, and at the age of less than 50 years, men are more affected than women, and women over 50 years old are affected more than men [3–5]. Knee osteoarthritis is one of the disability causes in the elderly. Patients with knee osteoarthritis suffer from progressive disability when walking up and down stairs [4–7]. The knee is the most common weight-bearing joint that is involved in osteoarthritis, and the incidence rate is 10 times higher on the knee's inner side than on the outer side [2–5]. Osteoarthritis may be primarily idiopathic or secondary to trauma, surgery, infection, or other diseases. Currently, no effective drug treatment can restore the original function and structure of damaged cartilage and other tissues involved in osteoarthritis or any other form of arthritis. Arthritis is managed in the usual way by controlling the symptoms of pain and immobility through non-steroidal anti-inflammatory painkillers. In research, it has been revealed that NSAIDs that are usually prescribed prevent cartilage matrix synthesis in humans, which in turn increases the destruction of joint cartilage in osteoarthritis [6–9]. Existing anti-inflammatory drugs have many side effects that sometimes lead to drug discontinuation. Hence, the finding of new drugs with fewer side effects is known as an important goal of researchers; herbal nanoparticles (NPs), which are more compatible with the human body and have acceptable diverse biological activities, can be considered a new class of drugs with significant advantages over chemical drugs [8–10].

Cyclodextrins (CDs) are known as cyclic compounds, which consist of glucopyranose units. Among cyclodextrins, α-, β-, and γ-CDs are the popular class of compounds that are different in the number of glucopyranose units (6 units for α-, 7 units for β-, and 8 units for γ-). The stereochemistry shows a torus-like molecular shape for CDs. This unique structure provides various applications for the compounds. CDs are utilized in food, pharmaceutics, biology, targeting drug delivery, and pollution removal [11–13]. The low water solubility, the appropriate cavity size, and no toxicity of β-CD make it the most usable compound compared to the other CDs [12]. The presence of 2 types of hydroxyl groups in the external layer of β-CD and the suitable size of the internal cavity of β-CD make it a convenient host to prepare inclusion complexes [12,14]. So far, β-CD has been utilized to encapsulate a range of chemical and natural products, including drugs and essential oils. Examples of these products include the essential oils of orange [15], yarrow [16], tea tree [17], *Thymus vulgaris* [18], as well as the drugs of fluconazole [19], resveratrol [20], and capecitabine [21]. Additionally, the β-CD complexes are found to have applications as catalysts and contamination removal [22–25].

The metallic ions play essential functions in all the life tissues from humans to microorganisms. The usage of metals to treat various diseases began in the early 1900s and it is continued to the present time [26]. Based on our literature analysis, numerous research teams have endeavored to green synthesize metallic NPs including gold, silver, palladium, zinc, titanium, nickel, manganese copper, and tin using plants as natural reducing and capping agents. Besides, the chemical, physical, biological, and medical properties of this class of NPs have been studied [27–35]. In contrast, the reports on the synthesis or complex preparation of metallic NPs using β-CD are limited. In the recent research, we focused on the synthesis of nickel NPs using β-CD for the first time. The NPs were identified by XRD, FT-IR, EDX, and FE-SEM. In the *in vivo* design, accelerating properties of the osteoarthritis articular cartilage repair of NiBCD NPs were determined.

2 Materials and methods

2.1 Synthesis procedure of NiBCD

A 0.2 g of β-CD was added to 10 mL of $NiNO_3$ (1.5×10^{-3}). The mixture was stirred for 1 day at 25°C. Then, the reaction mixture was sonicated at 45°C for 30 min. Next, the container was placed in the refrigerator for 24 h. After that, the mixture was centrifuged. The residues were washed with deionized water. Finally, the products were dried using an oven at 50°C. The NiBCD was formed in a dark green powder.

2.2 Osteoarthritis experiment

Sixty chicks, approximately 14 days old, were utilized in the study. Before commencing the experiment, the chicks were housed in standard laboratory conditions for 1 week. They had unrestricted access to food and water, and the temperature was maintained at 25°C. The chicks were kept in plastic containers. As per Wang et al., chondrocytes from the chick embryos articular cartilage were obtained through primary culture [3]. The chondrocytes underwent three passages before being utilized for the implementation process. The cell viability determination was indirectly established through the ratio of absorbance values between the control group and CGA-treated cells. Other studies have led to the creation of a chick injury model [3,4]. Initially, the xylazine intravenous injection was

used for anesthetizing the chicks. The right femur lateral condyle was then exposed under a stereoscope, followed by the creation of an osteochondral defect using a 21 G needle. The NiBCD NPs' (50 µg/mL) implantation was performed to address the osteochondral defects. The gait analysis was conducted 20 days post-operation. To distinguish between the injured left side foot and the control side (right) foot, the former was colored green while the latter was colored with black ink. The animals were then allowed to walk on white paper. Subsequently, evaluations were made regarding sway, stance, and stride lengths. After the study, the chicks were euthanized under anesthesia using 2% (v/v) isoflurane. After fixing the 10 samples of lateral femoral condyle articular surface in paraformaldehyde, the surgical procedure was performed on the distal femur lateral 1/3. This section was then removed and utilized to extract RNA and protein for more analysis in the case of the other five animals. The integral optical density (IOD) of PicroSirius red and Safranin O staining was determined and compared. The defect site was evaluated and quantified for blood vessel density (BSD) and cell numbers using Image Pro-Plus. Safranin O staining was assessed by the sulfated proteoglycans presence [4]. To create first-strand cDNA, the SuperScript III First-Strand Synthesis SuperMix was used, resulting in a final volume of 25 µL [3]. Subsequently, a polymerase chain reaction was performed. For Western blotting, the standard procedure was followed, utilizing antibodies [4].

2.3 Antioxidant efficacy

Within this method, different levels of NPs (ranging from 0 to 1,000 µg/mL) were combined with 1 mL of DPPH (300 µmol/l). The resultant blend was subsequently thinned with methanol until it reached a total volume of 4,000 µL.

Following incubation in the absence of light for a duration of 60 min, the absorbance at a wavelength of 517 nm was recorded. The percentage of DPPH radical inhibition was calculated using the formula provided in ref. [31].

$$\text{Seavenging activity (\%)} = \left(\frac{A_{517}\text{ of control} - A_{517}\text{ of sample}}{A_{517}\text{ of control}}\right) \times 100.$$

The sample absorption was indicated by A_{517} of the sample, whereas the control absorption was represented by A_{517} of the control.

2.4 Statistical analysis

Minitab software-21 was employed to evaluate the normality of the data. Following this, the non-normal outcomes were adjusted. Data variance analysis was carried out utilizing SPSS version 22 software, and Excel software was utilized to generate the graphs.

3 Results and discussion

3.1 Chemical characterization of NiBCD

The XRD analysis provides valuable information on the crystallinity of BCD complexes [36]. Figure 1 exhibits the XRD pattern of NiBCD NPs. The results suggest that NiBCD NPs are materialized in a fine crystalline powder. The signals at values of 26.76 (110), 37.41 (111), 43.47 (200), 63.22 (220), 75.76 (311), and 79.75 (222) are matched to standard JCDDS card No 1313-991, which belong to nickel oxide (NiO). The crystal size of NiBCD was measured by the Debye equation and found 31.85 nm.

The FT-IR spectroscopy qualitative analysis was run to evaluate the formation of NiBCD. The spectra of β-CD and NiBCD are indicated in Figure 2. The FT-IR spectrum of NiBCD is very similar to that of BCD. The peaks at 3,340, 2,943, 1,635, 1,415, 1,157 and 1,031 cm^{-1} are related to the O–H, C–H, β-CD, O–H, C–H, and C–O bonds as the common peaks in β-CD

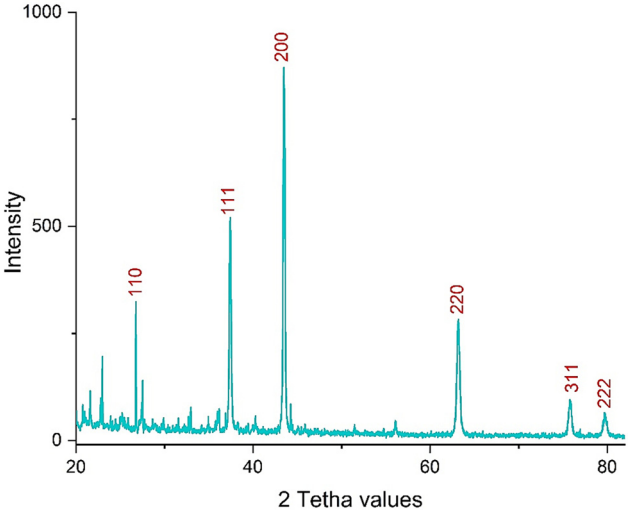

Figure 1: The XRD pattern of NiBCD.

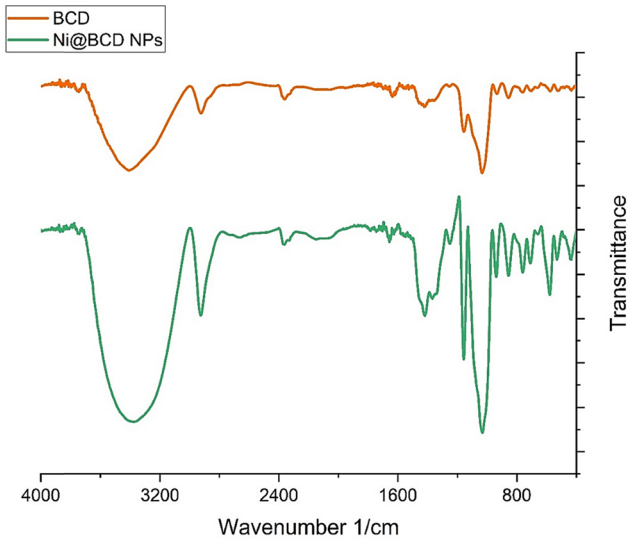

Figure 2: The FT-IR spectra of NiBCD and BCD.

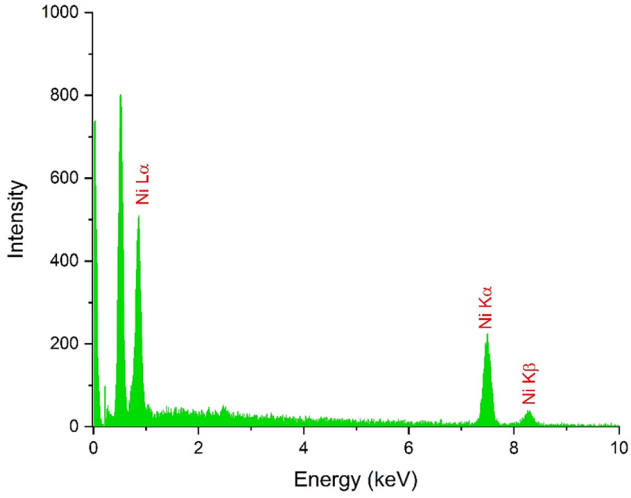

Figure 3: The EDX diagram of NiBCD.

H–O–H water deformation bands present in β-CD, 1,415 cm^{-1} belongs to in-plane bending vibration of O–H, 1,157 cm^{-1} attributed to overtone of C–H overtone stretching, and 1,031 cm^{-1} for the stretching vibrational band of C–O are the common peaks in β-CD that are matched to previous reports for FT-IR spectrum of β-CD [37,38]. For NiBCD NPs, all peaks of β-CD can be observed. Besides, according to previous studies, the vibration bands of Ni–O have been recorded in the region of 400–700 cm^{-1} [32,37,38]. In consequence, the other peaks in the NiBCD spectrum at 438, 530, 578, and 707 cm^{-1} are associated with Ni–O bonds for the nickel oxide or those of oxygen from the hydroxyl groups of BCD as the ligands to bind NiO. The FT-IR results of NiBCD and the starting material of β-CD approve that β-CD has performed a reducing function for the synthesis of NiBCD. Furthermore, the peaks NiBCD NPs approve the inclusion of complex formation by β-CD, which is shown in Scheme 1.

The elemental analysis of NiBCD NPs was evaluated by the qualitative analysis of the EDX method. The results are shown in Figure 3. The signals at the energy levels of 8.3, 7.5, and 0.87 keV are assigned for the electron migration of Ni Kβ, Ni Kα, and Ni Lα. Furthermore, the signals for the elements of oxygen and carbon of BCD appeared at 0.52 and 0.28 keV. These signals confirm the formation of the complex as well as the FT-IR results. Previous studies on the nickel oxide NPs' synthesis have reported similar EDX signals for nickel and oxygen [32,37,38].

The microscopic imaging technique, such as FE-SEM imaging, is known as an efficient method to evaluate the morphology of NPs. The FE-SEM image of NiBCD NPs is illustrated in Figure 4a and b. Based on the data, NiBCD

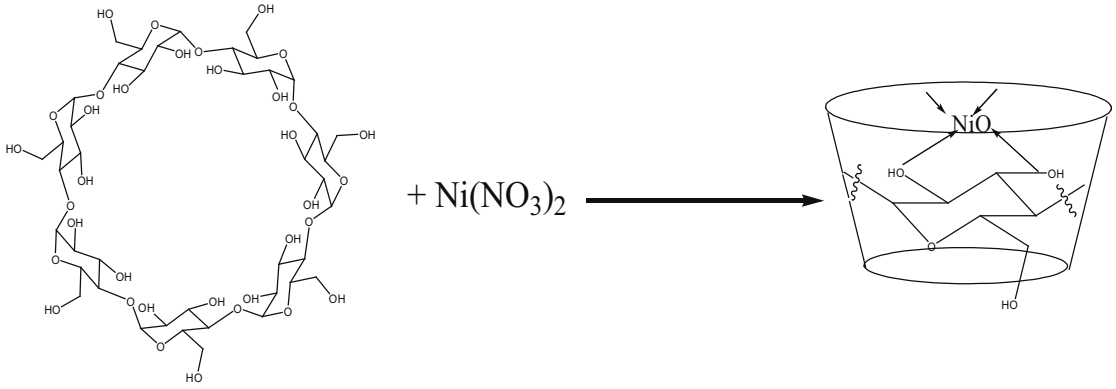

Scheme 1: The procedure synthesis of NiBCD NPs.

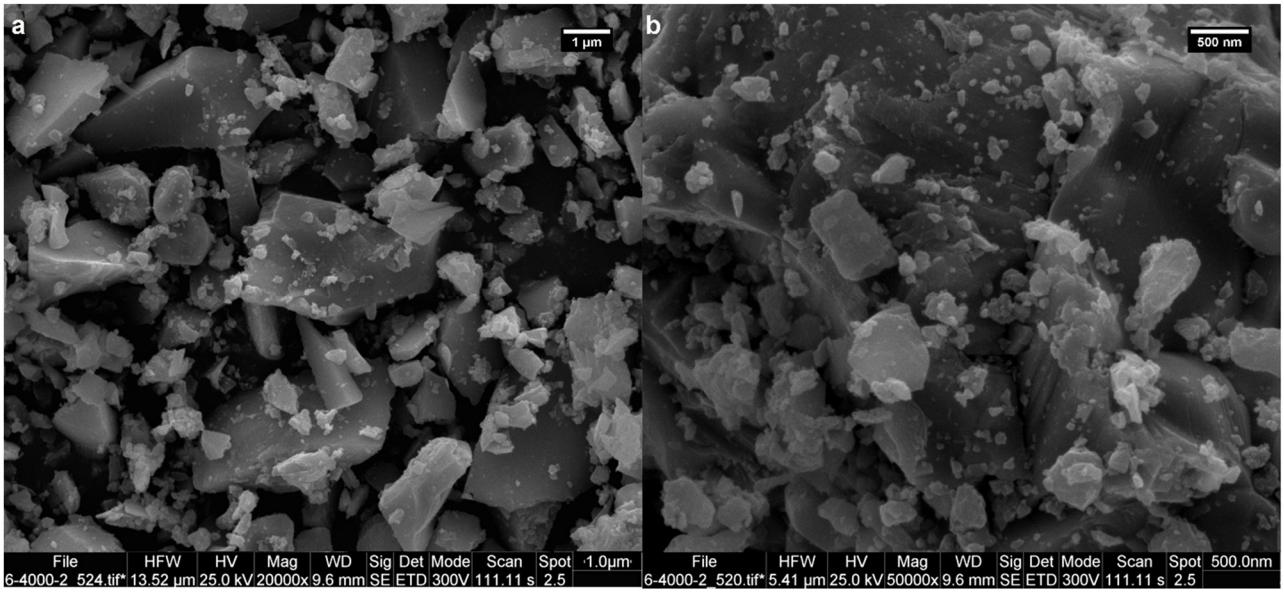

Figure 4: The FE-SEM images (a, b) of NiBCD NPs.

NPs have been formed in a non-spherical morphology with a size of less than 100 nm. Other research on the green synthesis of nickel NPs has presented an aggregation property for this class of material. In the opposite of these reports, NiBCD NPs do not show a strong tendency to aggregate.

3.2 Anti-osteoarthritic efficacy of NiBCD NPs

Nickel is widely recognized as a crucial element in the life cycles of plants, animals, and microorganisms. Its significance lies in its ability to activate carbon monoxide dehydrogenase, thereby facilitating the conversion of carbon monoxide into acetate in acetogenic bacteria. Additionally, Ni interacts with Fe in hemoglobin, aiding in the oxygen transportation. Furthermore, it plays a vital role in stimulating metabolism [39–42]. Moreover, nickel contributes to the genetic information encoded transmission in RNA and DNA. Lastly, it is present in the specific sugars enzyme matrix involved in metabolism. Nickel plays a crucial role in various physiological processes, including nerve impulse transmission, muscle contraction, and excitation. It achieves this by replacing

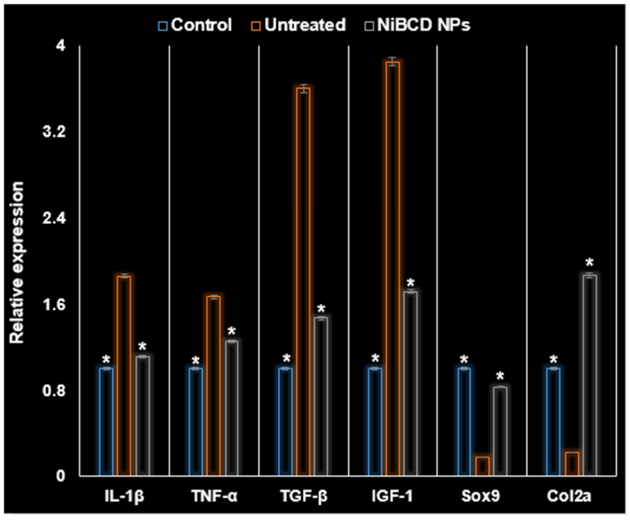

Figure 5: The activities of NiBCD NPs on the expressions of Sox9, IGF-1, TGF-β, TNF-α, IL-1β, and Col2a at the mRNA level.

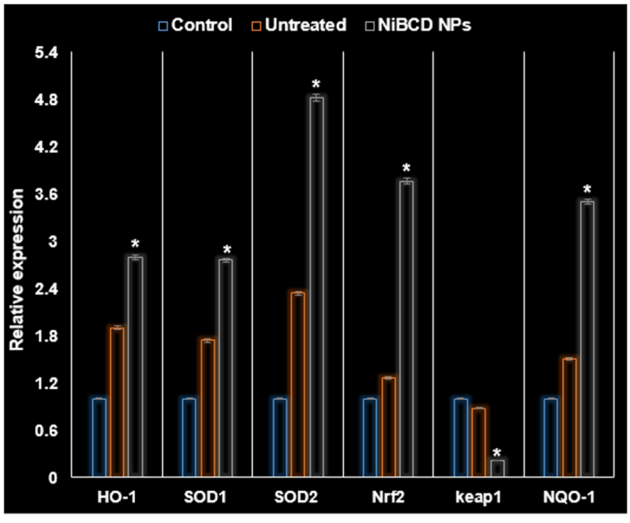

Figure 6: The activities of NiBCD NPs on the expressions of keap1, Nrf2, SOD2, SOD1, HO-1, and NQO-1 at the mRNA level.

calcium in the excitation process and participating in the binding with membrane ligands [41–43]. In rats, a deficiency of nickel has been observed to result in decreased iron levels in organs and a decline in hemoglobin, ultimately leading to the development of anemia. Nickel additionally functions as a cofactor in the activation of calcineurin, a phosphoprotein phosphatase that relies on calmodulin [42,43]. Furthermore, it plays a crucial role in regulating the production of cGMP, cardiovascular health, control of high blood pressure, and sperm physiology. Moreover, Ni is consistently found in RNA and forms bonds with serum albumins, proteins, and amino acids [41–43].

In this study, Figure 5 demonstrates that the mRNA levels of Sox9, IGF-1, TGF-β, TNF-α, IL-1β, and Col2a were significantly reduced ($P < 0.05$) by the NiBCD NPs compared to the untreated group. Moreover, the mRNA levels of keap1, Nrf2, SOD2, SOD1, NQO-1, and HO-1 were significantly increased ($P < 0.05$) by the NiBCD NPs compared to both the control and untreated groups. However, there was no significant difference ($P < 0.05$) in the expressions

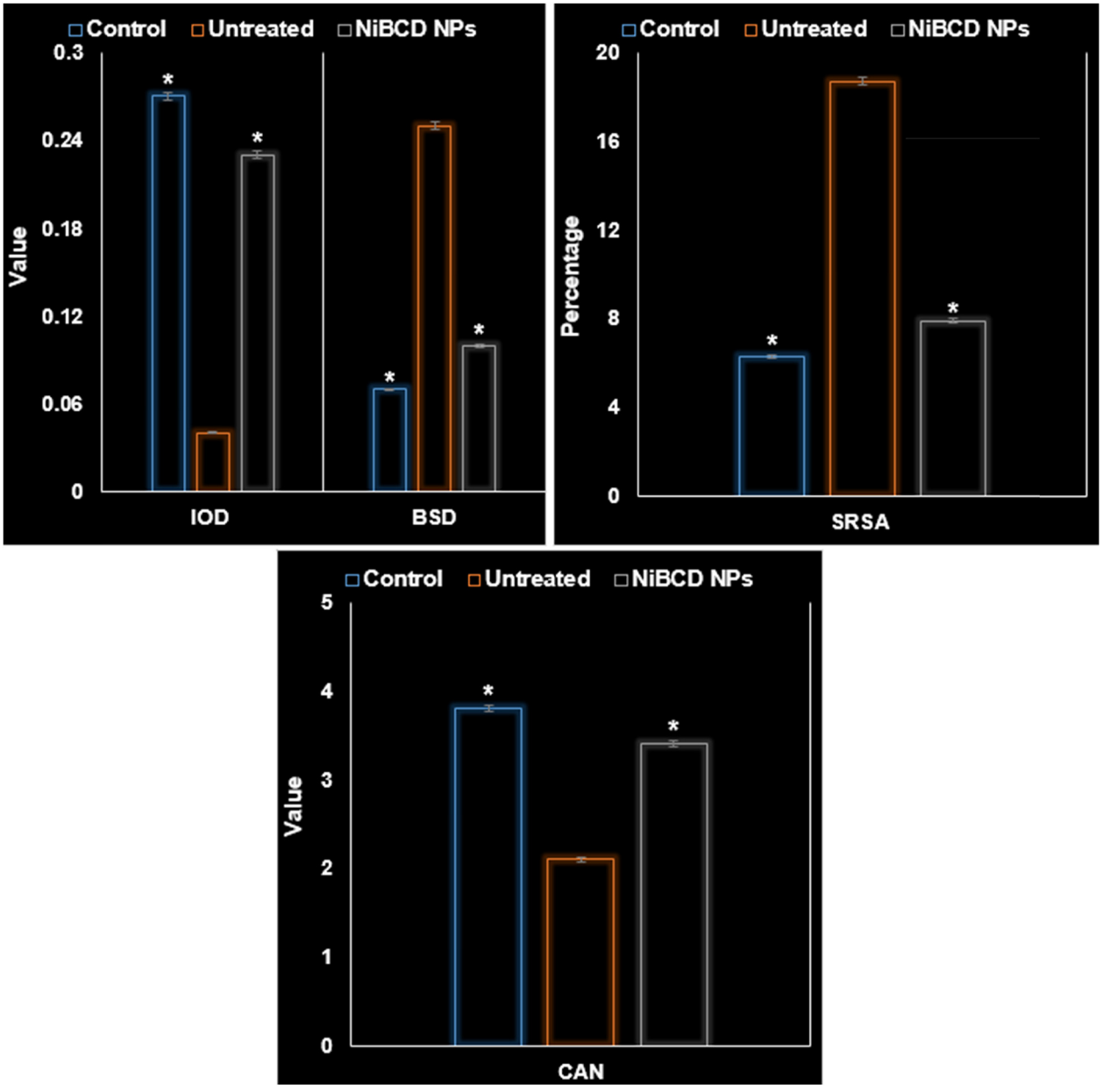

Figure 7: The activities of NiBCD NPs on ACN, SRSA, BSD, and IOD of the articular cartilage.

of Sox9, IGF-1, TGF-β, TNF-α, Col2a, and IL-1β between the control and NiBCD NP groups, as shown in Figure 6.

The untreated group showed a decrease in the BSD and IOD of the articular cartilage, along with an increase in the average cell numbers in isogenous groups of chondrocytes (ACN) and SRSA. In contrast, the NiBCD NPs had the opposite effect, increasing the BSD and IOD while decreasing the ACN and SRSA ($P < 0.05$) (Figure 7).

According to the findings presented in Figure 8, the protein level analysis revealed that the NiBCD NPs led to a decrease in the expressions of p-p65 and MMP-13 ($P < 0.05$). No significant difference ($P < 0.05$) was reported in these parameters between the control and NiBCD NP groups.

According to the findings presented in Figure 9, it can be observed that the NiBCD NPs exhibited a significant increase in both the fluorescent intensity of F-actin and the $pHIS3^+$ cells ($P < 0.05$).

On day 20, the untreated group revealed no significant difference ($P < 0.05$) in terms of footprint area (cm^2), sway length (cm), stance length (cm), and stride length (cm) compared to the NiBCD NPs and control groups. However, the NiBCD NPs demonstrated an increase in these parameters, including footprint area (cm^2), sway length (cm), stance length (cm), and stride length (cm), as shown in Figure 10.

Furthermore, the application of NiBCD NPs resulted in a dose-dependent increase in the cell viability rate (CVR) as observed in the cell counting kit-8 assay (Figure 11).

The activation of the inflammasome plays a significant role in the various diseases development, including pulmonary fibrosis, type II diabetes, gout, atherosclerosis, and osteoarthritis. Macrophages, as the body's primary defense mechanism, are responsible for processing NPs and facilitating the targeting of macrophages by nanomaterials, which distinguishes them from small molecule drugs [44]. In the preceding investigation, Jin et al. (2023) discovered that the inhibition of inflammasome assembly can be effectively achieved by Ni NPs. Specifically, they observed the inhibition of NLRP3, NLRC4, and AIM2 inflammasomes. Furthermore, their research demonstrated that Ni NPs can impede neutrophil recruitment in a mouse model of acute peritonitis and alleviate symptoms in a colitis mouse model. The underlying mechanism behind these effects was identified as the inhibition of IL-1β maturation. This finding stands in stark contrast to previous studies suggesting that inorganic NPs typically induce inflammasome activation. Instead, Jin et al. provide evidence that inorganic NPs themselves possess the ability to inhibit the activation of various inflammasome types. Ni NPs have shown their ability to effectively inhibit the activation of

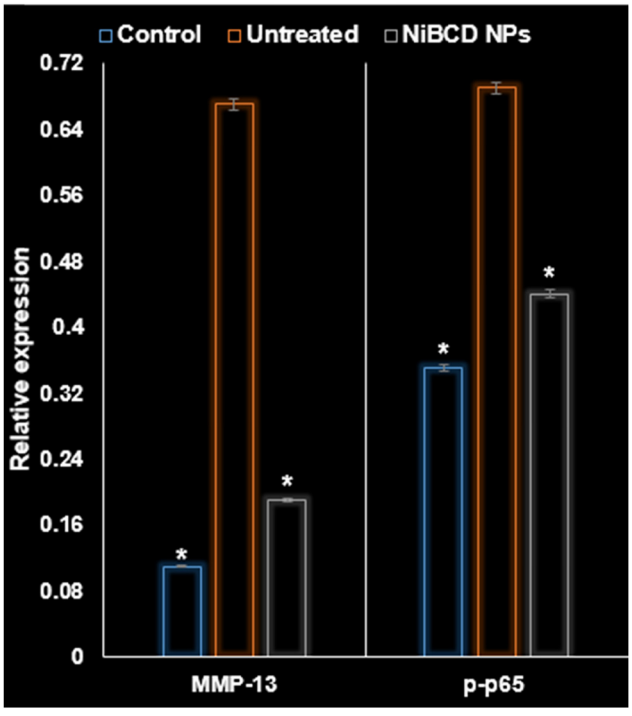

Figure 8: The activities of NiBCD NPs on the expressions of p-p65 and MMP-13 at the protein level.

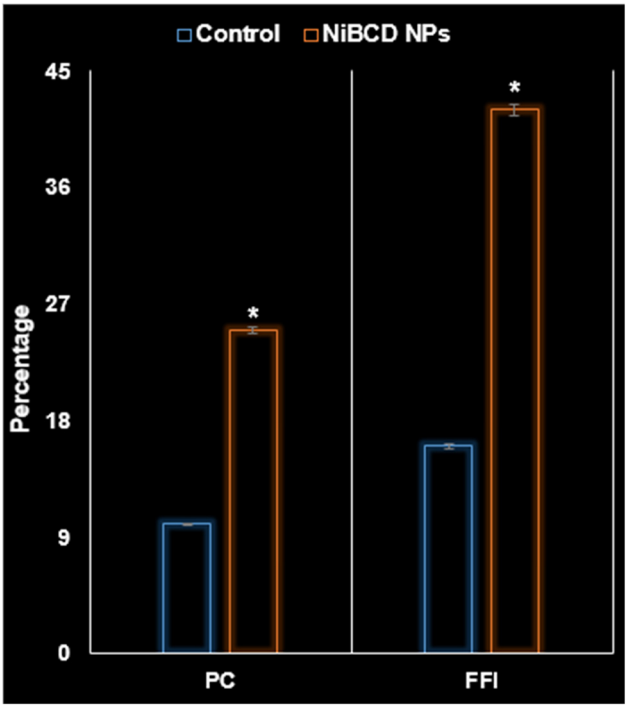

Figure 9: The activities of NiBCD NPs on F-actin fluorescent intensity (FFI) and $pHIS3^+$ cells (PC).

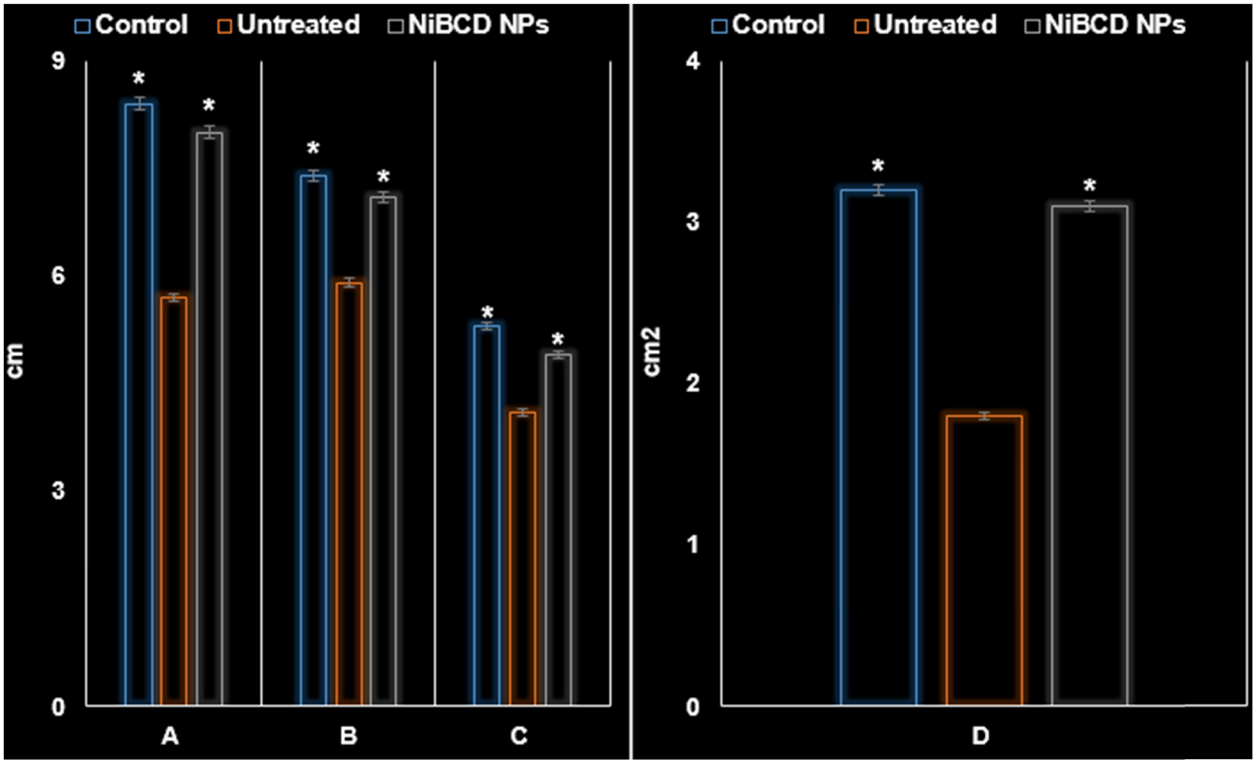

Figure 10: The activities of NiBCD NPs on several parameters on day 20. A: stride length. B: stance length. C: sway length. D: footprint area of the injured side.

inflammasomes by suppressing Neat1. Further investigation is required to understand the precise mechanism through which Ni NPs regulate Neat1 transcription. If successful, this research could potentially address the existing challenge of limited inflammasome activation in engineered NP applications by developing Ni NPs with enhanced biocompatibility [44].

The enhanced anti-inflammatory efficacy in this research was achieved through the combined effectiveness of β-cyclodextrin and nickel. The primary reason behind this outcome was the increase in surface/volume, resulting in an atom's greater influence on the particle's surface compared to its interior. The result of this phenomenon is a rise in the surface energy [45]. The surface area expansion of NiNPs facilitates optimal interaction between β-cyclodextrin and the receptor site, resulting in its therapeutic benefits. This process typically reduces systemic inflammation and concurrently promotes the growth of peripheral blood lymphocytes, thereby augmenting the natural killer cells' cytotoxic effectiveness [45].

3.3 Antioxidant efficacy of NiBCD NPs

The outcomes derived from the DPPH assay illustrated a rise in the inhibition rate with the escalation of NiBCD NP

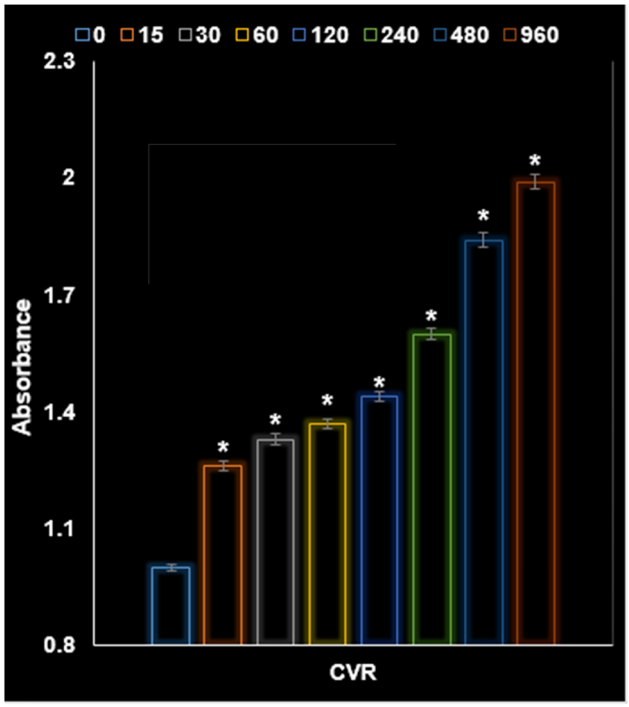

Figure 11: The activities of NiBCD NPs on CVR in the cell counting kit-8 assay.

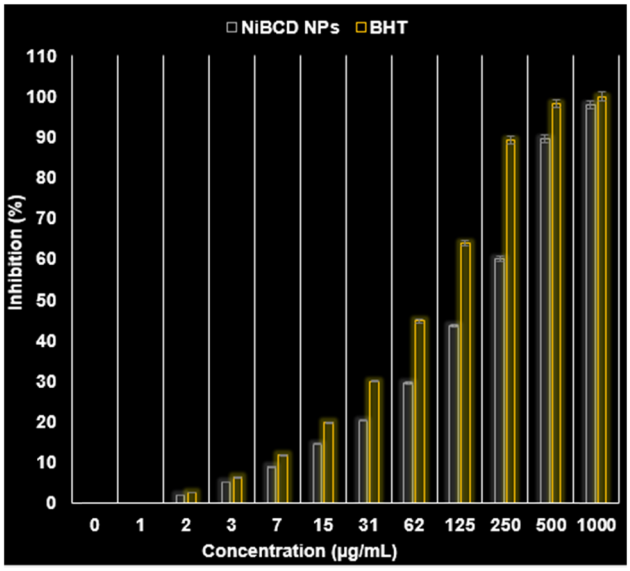

Figure 12: The antioxidant activities of NiBCD NPs.

concentration. Throughout this study, NiBCD NPs displayed the greatest antioxidant effectiveness at 1,000 µg/mL, showcasing an inhibition rate of around 100%. The NiBCD NPs exhibited an antioxidant IC50 value of 173 µg/mL, whereas the standard positive control or BHT showed a value of 78 µg/mL. The results of the antioxidant assay can be observed in Figure 12.

4 Conclusion

The structure of BCD provides a great ability for molecules to use as a sufficient host to prepare inclusion complexes of different compounds such as drugs or catalysts. In the present research, the nickel oxide NPs were synthesized using BCD as a capping and reducing agent. The NiBCD was materialized in the formula of NiO. The FT-IR results approved the binding of NiO to BCD as well as the XRD and EDX diagrams. The levels of MMPs, p-p65, TNF-α, and IL-1β expression were reduced by the NiBCD NPs. The presence of these NPs in the histological assay resulted in chondrocyte proliferation and increased cartilage matrix synthesis, as well as decreased abnormal vasculature formation. It was discovered that the NPs' application accelerated the recovery of injury-induced dysfunction. Furthermore, we demonstrated the positive effectiveness of NiBCD NPs in stimulating chondrogenesis. The application of the NPs also suppressed angiogenesis and abnormal fibrosis at the injury site. Based on the results of clinical trial studies, these recent NPs may serve as a novel drug for expediting osteoarthritis articular cartilage repair.

Funding information: This research received no external funding.

Author contributions: Fengkun Ji: conceptualization, investigation, methodology, project administration, resources, software, supervision, writing – original draft, and writing – review and editing. Xu Zeng: conceptualization, investigation, project administration, resources, supervision, validation, writing – original draft, and writing – review and editing. Zhendong Wang: formal analysis, acquisition, investigation, methodology, project administration, resources, software, supervision, validation, and visualization. Hui Chen: investigation, methodology, project administration, resources, software, supervision, validation, visualization, writing – original draft, and writing – review and editing. Wenchao Li: conceptualization, acquisition, investigation, methodology, project administration, and resources. Haoyu Li: conceptualization, data curation, formal analysis, acquisition, investigation, validation, visualization, writing – original draft, and writing – review and editing.

Conflict of interest: The authors declare no conflict of interest.

Ethical approval: The conducted research is not related to either human or animal use.

Data availability statement: All data generated or analyzed during this study are included in this published article.

References

[1] Pereira D, Peleteiro B, Araujo J, Branco J, Santos RA, Ramos E. The effect of osteoarthritis definition on prevalence and incidence estimates: a systematic review. Osteoarthr Cartil. 2011;19:1270–85.
[2] Hunter DJ, Schofield D, Callander E. The individual and socioeconomic impact of osteoarthritis. Nat Rev Rheumatol. 2014;10:437–41.
[3] Wang P, Zhang F, He Q, Wang J, Shiu HT, Shu Y, et al. Flavonoid compound icariin activates hypoxia inducible factor-1alpha in chondrocytes and promotes articular cartilage repair. PLoS one. 2016;11(2):e0148372.
[4] Cheng X, Li K, Xu S, Li P, Yan Y, Wang G, et al. Applying chlorogenic acid in an alginate scaffold of chondrocytes can improve the repair of damaged articular cartilage. PLoS ONE. 2018;13(4):e0195326.
[5] Sharma L, Song J, Felson DT, Cahue S, Shamiyeh E, Dunlop DD. The role of knee alignment in disease progression and functional decline in knee osteoarthritis. JAMA. 2001;286:188–95.
[6] Katz JN, Arant KR, Loeser RF. Diagnosis and treatment of hip and knee osteoarthritis: a review. JAMA. 2021;325:568–78.
[7] Lieberthal J, Sambamurthy N, Scanzello CR. Inflammation in joint injury and post-traumatic osteoarthritis. Osteoarthr Cartil. 2015;23:1825–34.

[8] Sommer OJ, Kladosek A, Weiler V, Czembirek H, Boeck M, Stiskal M. Rheumatoid arthritis: a practical guide to state-of-the-art imaging, image interpretation, and clinical implications. Radiographics. 2005;25:381–98.
[9] Blass S, Engel JM, Burmester GR. The immunologic homunculus in rheumatoid arthritis. Arthritis Rheum. 1999;42:2499–2506.
[10] Wen J, Li H, Dai H, Hua S, Long X, Li H, et al. Intra-articular nanoparticles based therapies for osteoarthritis and rheumatoid arthritis management. Mater Today Bio. 2023 Feb 26;19:100597.
[11] Ramasamy S, Enoch IV, Rajkumar SRJ. Polymeric cyclodextrin-dextran spooled nickel ferrite nanoparticles: Expanded anticancer efficacy of loaded camptothecin. Mater Lett. 2020;261:127114.
[12] Dehghani A, Bahlakeh G, Ramezanzadeh B. Beta-cyclodextrin-zinc acetylacetonate (β-CD@ ZnA) inclusion complex formation as a sustainable/smart nanocarrier of corrosion inhibitors for a water-based siliconized composite film: Integrated experimental analysis and fundamental computational electronic/atomic-scale simulation. Compos Part B: Eng. 2020;197:108152.
[13] Payamifar S, Poursattar Marjani A. A new β-cyclodextrin-based nickel as green and water-soluble supramolecular catalysts for aqueous Suzuki reaction. Sci Rep. 2023;13(1):21279.
[14] Huff C, Long JM, Abdel-Fattah TM. Beta-cyclodextrin-assisted synthesis of silver nanoparticle network and its application in a hydrogen generation reaction. Catalysts. 2020;10(9):1014.
[15] Li D, Wu H, Huang W, Guo L, Dou H. Microcapsule of sweet orange essential oil encapsulated in beta-cyclodextrin improves the release behaviors in vitro and in vivo. Eur J Lipid Sci Technol. 2018;120(9):1700521.
[16] Rakmai J, Cheirsilp B, Torrado-Agrasar A, Simal-Gándara J, Mejuto JC. Encapsulation of yarrow essential oil in hydroxypropyl-beta-cyclodextrin: physiochemical characterization and evaluation of bio-efficacies. CyTA-J Food. 2017;15(3):409–17.
[17] Shrestha M, Ho TM, Bhandari BR. Encapsulation of tea tree oil by amorphous beta-cyclodextrin powder. Food Chem. 2017;221:1474–83.
[18] Arrais A, Bona E, Todeschini V, Caramaschi A, Massa N, Roncoli M, et al. Thymus vulgaris essential oil in beta-cyclodextrin for solid-state pharmaceutical applications. Pharmaceutics. 2023;15(3):914.
[19] Malaquias LF, Sa-Barreto LC, Freire DO, Silva IC, Karan K, Durig T, et al. Taste masking and rheology improvement of drug complexed with beta-cyclodextrin and hydroxypropyl-β-cyclodextrin by hot-melt extrusion. Carbohydr Polym. 2018;185:19–26.
[20] Iskineyeva A, Fazylov S, Bakirova R, Sarsenbekova A, Pustolaikina I, Seilkhanov O, et al. Combined In Silico and Experimental Investigations of Resveratrol Encapsulation by Beta-Cyclodextrin. Plants. 2022;11(13):1678.
[21] Ameli H, Alizadeh N. Targeted delivery of capecitabine to colon cancer cells using nano polymeric micelles based on beta cyclodextrin. RSC Adv. 2022;12(8):4681–91.
[22] Guo R, Wang R, Yin J, Jiao T, Huang H, Zhao X, et al. Fabrication and highly efficient dye removal characterization of beta-cyclodextrin-based composite polymer fibers by electrospinning. Nanomaterials. 2019;9(1):127.
[23] Sulaiman NS, Zaini MAA, Arsad A. Evaluation of dyes removal by beta-cyclodextrin adsorbent. Mater Today: Proc. 2021;39:907–10.
[24] Poór M, Faisal Z, Zand A, Bencsik T, Lemli B, Kunsági-Máté S, et al. Removal of zearalenone and zearalenols from aqueous solutions using insoluble beta-cyclodextrin bead polymer. Toxins. 2018;10(6):216.
[25] Ndlovu LN, Malatjie KI, Chabalala MB, Mishra AK, Mishra SB, Nxumalo EN. Beta cyclodextrin modified polyvinylidene fluoride adsorptive mixed matrix membranes for removal of Congo red. J Appl Polym Sci. 2022;139(23):52302.
[26] Oliveri V, Pietropaolo A, Sgarlata C, Vecchio G. Zinc complexes of cyclodextrin-bearing 8-hydroxyquinoline ligands: a comparative study. Chem–An Asian J. 2017;12(1):110–5.
[27] Elia P, Zach R, Hazan S, Kolusheva S, Porat ZE, Zeiri Y. Green synthesis of gold nanoparticles using plant extracts as reducing agents. Int J Nanomed. 2014;9:4007–21.
[28] Srikar SK, Giri DD, Pal DB, Mishra PK, Upadhyay SN. Green synthesis of silver nanoparticles: a review. Green Sustain Chem. 2016;6(1):34–56.
[29] Gulbagca F, Aygün A, Gülcan M, Ozdemir S, Gonca S, Şen F. Green synthesis of palladium nanoparticles: Preparation, characterization, and investigation of antioxidant, antimicrobial, anticancer, and DNA cleavage activities. Appl Organomet Chem. 2021;35(8):e6272.
[30] Mahdavi B, Saneei S, Qorbani M, Zhaleh M, Zangeneh A, Zangeneh MM, et al. Ziziphora clinopodioides Lam leaves aqueous extract mediated synthesis of zinc nanoparticles and their antibacterial, antifungal, cytotoxicity, antioxidant, and cutaneous wound healing properties under in vitro and in vivo conditions. Appl Organomet Chem. 2019;33(11):e5164.
[31] Seydi N, Mahdavi B, Paydarfard S, Zangeneh A, Zangeneh MM, Najafi F, et al. Preparation, characterization, and assessment of cytotoxicity, antioxidant, antibacterial, antifungal, and cutaneous wound healing properties of titanium nanoparticles using aqueous extract of Ziziphora clinopodioides Lam leaves. Appl Organomet Chem. 2019;33(9):e5009.
[32] Huang Y, Zhu C, Xie R, Ni M. Green synthesis of nickel nanoparticles using Fumaria officinalis as a novel chemotherapeutic drug for the treatment of ovarian cancer. J Exp Nanosci. 2021;16(1):368–81.
[33] Mahdavi B, Paydarfard S, Zangeneh MM, Goorani S, Seydi N, Zangeneh A. Assessment of antioxidant, cytotoxicity, antibacterial, antifungal, and cutaneous wound healing activities of green synthesized manganese nanoparticles using Ziziphora clinopodioides Lam leaves under in vitro and in vivo condition. Appl Organomet Chem. 2020;34(1):e5248.
[34] Gu J, Aidy A, Goorani S. Anti-human lung adenocarcinoma, cytotoxicity, and antioxidant potentials of copper nanoparticles green-synthesized by Calendula officinalis. J Exp Nanosci. 2022;17(1):285–96.
[35] Shu M, Mahdavi B, Balčiūnaitienė A, Goorani S, Mahdavi AA. Novel green synthesis of tin nanoparticles by medicinal plant: Chemical characterization and determination of cytotoxicity, cutaneous wound healing and antioxidant properties. Micro Nano Lett. 2023;18(2):e12157.
[36] Cheng X, Lu Z, Li Y, Wang Q, Lu C, Meng Q. An interesting molecular-assembly of β-cyclodextrin pipelines with embedded hydrophilic nickel maleonitriledithiolate. Dalton Trans. 2011;40(44):11788–94.
[37] David I, Orboi MD, Simandi MD, Chirilă CA, Megyesi CI, Rădulescu L, et al. Fatty acid profile of Romanian's common bean (Phaseolus vulgaris L.) lipid fractions and their complexation ability by β-cyclodextrin. PLoS One. 2019;14(11):e0225474.
[38] Rachmawati H, Edityaningrum CA, Mauludin R. Molecular inclusion complex of curcumin–β-cyclodextrin nanoparticle to enhance curcumin skin permeability from hydrophilic matrix gel. Aaps Pharmscitech. 2013;14:1303–12.

[39] Mahdavi B, Paydarfard S, Rezaei-Seresht E, Baghayeri M, Nodehi M. Green synthesis of NiONPs using Trigonella subenervis extract and its applications as a highly efficient electrochemical sensor, catalyst, and antibacterial agent. Appl Organomet Chem. 2021;35(8):e6264.
[40] Karimian M, Abbasi N, Ghaneialvar H, Karimi E. Green synthesis of NiO nanoparticles using Calendula officinalis extract: Chemical charactrization, antioxidant, cytotoxicity, and anti-esophageal carcinoma properties. Arab J Chem. 2021;14(5):103105.
[41] Cemple M, Nickel G. Nickel: A review of its sources and environmental toxicology. Pol J Env Stud. 2006;15:375–82.
[42] Chohan ZH, Sherazi SKA. Biological role of cobalt (II), copper (II) and nickel (ii) metal ions on the antibacterial properties of some nicotinoyl-hydrazine derived compounds. Met Based Drugs. 1997;4:69–74.
[43] Thauer RK, Diekert G, Schonheit P. Biological role of nickel. Trends Biochem Sci. 1980;5:304–6.
[44] Lin J, Dong L, Liu YM, Hu Y, Jiang C, Liu K, et al. Nickle-cobalt alloy nanocrystals inhibit activation of inflammasomes. Natl Sci Rev. 2023 Jun 26;10(8):nwad179.
[45] Angajala G, Radhakrishnan S. A review onnickel nanoparticles as effective therapeutic agents forinflammation. Inflamm Cell Signal. 2014;1:e271.